P-08-42

Oskarshamn site investigation

Mineralogy in water conducting zones

Results from boreholes KLX07A+B and KLX08

Henrik Drake, Isochron GeoConsulting HB
Eva-Lena Tullborg, Terralogica AB

July 2008

Svensk Kärnbränslehantering AB
Swedish Nuclear Fuel
and Waste Management Co

Box 250, SE-101 24 Stockholm
Phone +46 8 459 84 00

ISSN 1651-4416
SKB P-08-42

Oskarshamn site investigation

Mineralogy in water conducting zones

Results from boreholes KLX07A+B and KLX08

Henrik Drake, Isochron GeoConsulting HB
Eva-Lena Tullborg, Terralogica AB

July 2008

Keywords: Water conducting zones, Mineralogy, Chemistry, X-ray diffraction, SEM-EDS, Stable isotopes, U–series disequilibrium, Laxemar.

Abstract

This report is a part of the SKB site investigations in Oskarshamn and reports results from detailed studies of fracture coatings/fillings from water conducting sections (sections sampled for complete chemical characterisation) in borehole KLX08 in the Laxemar subarea. Two samples from borehole KLX07A+B are also included in this report. Methods used are mineral identification (XRD, SEM-EDS), chemistry (ICP-AES/QMS), isotope ratios (U-Series disequilibrium, $\delta^{13}C$, $\delta^{18}O$). The results presented in this report constitute only a minor part of all the fracture mineral analyses carried out within the investigation program for the entire Oskarshamn site investigation area and therefore no thorough interpretations are included in this P-report.

Sammanfattning

Denna rapport ingår i SKB:s platsundersökningar i Oskarshamnsområdet. I rapporten presenteras resultat från detaljerade undersökningar av sprickfyllningar/beläggningar i vattenförande zoner (sektioner provtagna för fullständig kemikaraktärisering) i borrhål KLX08. Två prover från KLX07A+B är också inkluderade i denna rapport. Metoder som använts är mineralidentifikation (SEM-EDS, XRD), kemi (ICP-AES/QMS), isotopkvoter (U-serien, $\delta^{13}C$, $\delta^{18}O$). De resultat som presenteras här utgör endast en bråkdel av de sprickmineralogiska analyser som utförts inom Oskarshamns platsundersökningsområde. Inga omfattande tolkningar av data redovisas därför i denna rapport.

Contents

1 Introduction

This document reports results from detailed studies of fracture coatings/fillings from water conducting sections of which 3 coincides with sections sampled for complete chemical characterisation in borehole KLX08 in the Laxemar subarea. Two samples from borehole KLX07A+B are also included in this report. In Table 1-1 controlling documents for performing this activity are listed. Both the activity plan and the method description are SKB's internal controlling documents. The location of the boreholes is shown in Figure 1-1.

Table 1-1. Controlling documents for the performance of the activity.

Activity plan	**Number**	**Version**
Sprickmineralogiska undersökningar i KLX07 (A+B), KLX08 och KLX10	AP-PS-400-05-074	1.0
Method descriptions	**Number**	**Version**
Sprickmineralanalys	SKB MD 144.001	1.0

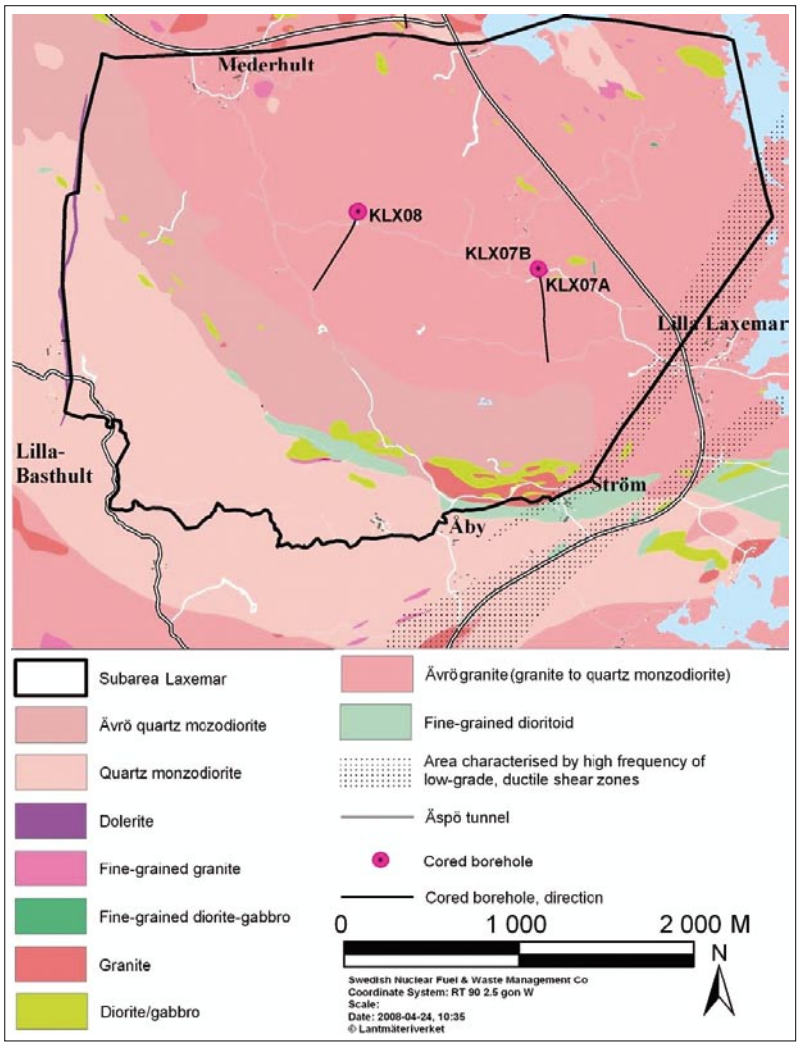

Figure 1-1. *Geological map of the Laxemar subarea with the investigated boreholes KLX07A+B and KLX08 shown.*

2 Objective and scope

The objective and scope has been to investigate the mineralogy (with SEM-EDS and XRD), chemistry (with ICP-AES/QMS) and isotope characteristics ($\delta^{13}C$, $\delta^{18}O$ and U-series disequilibrium analysed with mass spectrometry) of sections sampled for complete chemical characterisation in borehole KLX08, Laxemar subarea. Two additional samples from borehole KLX07A+B are also included. The task has been to:

- Identify minerals; the drill core mapping is based on macroscopic determination of fracture minerals and SEM-analysis or XRD is needed to give a more detailed and precise description of the mineralogy in water conducting sections.
- Give input to hydrogeochemical modelling and give a background to paleohydrogeological interpretations.

3 Equipment

3.1 Description of equipment

The following equipment was used in the investigations:

- Scanning electron microscope (Hitachi S-3400N) with EDS (Oxford Instruments).
- Stereo microscope (Leica MZ12).
- Digital camera (Konica Revio KD-420Z).
- Rock saw.
- Rock Labs swing mill.
- Knife.
- Magnifying lens – 10x.
- Scanner (Epson 3200).
- Computer software, e.g. Corel Draw 11, Microsoft Word, Microsoft Excel, Link ISIS.
- Mass-spectrometer.

All equipment listed above is property of Earth Sciences Centre, University of Gothenburg, or the authors. For equipment used for whole rock chemistry analyses, U-series analyses, X-ray diffraction and stable isotope analyses, see Chapter 4.

4 Execution

4.1 Sample collection and preparations

Samples were collected from the drill cores KLX08 and KLX07A+B and, in order to sample water conducting sections, the flow logs from each boreholes were used as reference /Sokolnicki and Pöllänen 2005; Sokolnicki and Rouhiainen 2005/. Unfortunately, some water conducting zones (e.g. in KLX10) did not include suitable samples whereas some less conductive sections provided some samples of interest and therefore scattered samples throughout the drill core were collected. The samples were then photographed.

The fracture surfaces of most of the samples were removed, by sawing if needed. The fracture surfaces samples were glued to a plastic plate, in order to obtain a horizontal surface. The fracture surfaces were then scanned as a support to the SEM investigations. The samples were then investigated with SEM-EDS, in order to identify the major minerals (as well as some minor and accessory minerals) and to characterise the fracture surface morphology.

After this procedure, the minerals on the fracture surfaces of the samples were scraped off using a knife. The scrape off material was sewed and the material with a grain size smaller than 0.125 mm was collected for U-series analysis. The rest of the material was milled to a grain size smaller than 0.125 mm. The major part of the powdered material was then added to the material collected for U-series analyses and the remaining material was used for ICP-AES and ICP-QMS chemical analyses and X-ray diffraction (if enough material).

Samples including a significant amount of calcite were investigated with a hand lens, stereo microscope and SEM, in order to make out the crystal morphology, if possible. The calcite crystals were then scraped off with a knife and this material was checked for purity in stereo microscope and then analysed for stable isotopes $\delta^{18}O$ and $\delta^{13}C$. Investigation methods used for each sample are listed in Table 4-1.

Table 4-1. Investigation methods used for each sample

Borehole and section (m)*	Sample (m)	ICP-AES/QMS	XRD	U-series	$\delta^{13}C$ and $\delta^{18}O$	Surface sample
KLX07B						
	4.85–4.85	X	X	X		X
KLX07A						
	782.64–782.83	X	X	X		X
KLX08						
	106.33–106.40	X	X	X		X
	121.57–121.62	X	X	X	X	X
197–206.6*	198.97–199.10	X		X		X
	218.80–218.83	X	X	X		X
	347.99–348.15					X
396–400.87*	no sample					
	408.11–408.17	X	X	X		
	465.10–465.14	X		X		X
476–485.65*	478.44–478.59	X	X	XX	X	X
610–619.65*	614.47–614.72	X	X	XX		X
	772.34–772.49	X	X	XX		X
	852.29–852.40				X	X
	852.67–852.74				X	X

* Sections sampled for complete chemical characterisation.

4.2 SEM-EDS analyses

The SEM investigations and EDS microanalyses were carried out on an Oxford Instruments Energy Dispersive System mounted on a Hitachi S-3400N scanning electron microscope at the Earth Sciences Centre, University of Gothenburg, Sweden. The acceleration voltage was 20 kV, the working distance 10 mm and the specimen current was about 1nA. The investigations were carried out using low vacuum mode (20 Pa). The instrument was calibrated at least twice every hour using a cobalt standard linked to simple oxide and mineral standards, to confirm that the drift was acceptable. X-ray spectrometric corrections were made by an on-line computer system. Proper mineral analyses were not carried out due to the uneven surface of the samples which cause too low total values (a polished surface is needed). The mineralogy (except for clay minerals) was identified based on element ratios and spectra of each element of the different minerals.

4.3 ICP-AES, ICP-QMS

ICP-AES/ICP-QMS analyses were carried out by Analytica AB. For most elements the following procedure was applied: 0,125 g sample is fused with 0.375 g $LiBO_2$ and dissolved in dilute HNO_3. However, for Co, Cu, Ni and Zn analyses, digestion was done by microwave heating in closed teflon vessels with HNO_3/H_2O 1:1. LOI (Loss on ignition) is carried out at 1,000°C (some samples were too small to perform LOI). Concentrations of the elements are determined by ICP-AES and ICP-QMS. Analyses are carried out according to EPA methods (modified) 200.7 (ICP-AES) and 200.8 (ICP-QMS).

4.4 X-ray diffraction

Samples > 0.40 g were divided with a sample separator and one of the two parts was milled in an agate mortar. All the material from samples < 0.40 g were milled to a fine powder and packed in a small sampler for XRD-analysis and identification of major minerals. Extremely small samples was put on a silicon plate and suspended in alcohol to spread it over the whole plate. The sample was then dried and XRD-analysis could then be performed on the sample.

The analyses were carried out by SGU, Uppsala, Sweden, according to the following procedure. The fine-fraction (< 35 μm) of each sample was dispersed in distilled water, filtered and oriented according to /Drever 1973/. In samples of small volumes the suspension was repeatedly put on glass and dried. Three measurements were carried out on each of the fine fraction samples for clay mineral identification; 1) dried samples 2) saturated with ethyleneglycol for two hours and finally 3) after heating to 400°C in two hours. Coarser material was wet sieved and dried. The > 35μm fraction was ground by hand in an agate mortar. The sample powder was randomly orientated in the sample holder (and very small sample volumes on a piece of glass). The radiation (CuK_α) in the diffractometer was generated at 40 kV and 40 mA, and the X-rays were focussed with a graphite monochromator. Scans were run from 2°–65° (2-theta) or from 2°–35° (samples with preferred crystal orientation) with step size 0.02° (2-theta) and counting time 1 s $step^{-1}$. The analyses were performed with a fixed 1° divergence and a 2 mm receiving slit. The XRD raw files were taken up in the Bruker/Siemens $DIFFRAC^{PLUS}$ software (version 2.2), and evaluated in the programme EVA. The minerals were identified by means of the /PDF 1994/ computer database. Additional data from /Brindley and Brown 1984; Jasmund and Lagaly 1993/ was used for clay mineral identification.

4.5 U-series analyses

The Uranium-Thorium analyses were carried out at the Scottish Universities Environmental Research Centre, Scotland, accordingly: Sample material was furnaced at 600°C (in increments of 100°C if material is highly organic). The material was washed from the crucible with H_2O into a beaker, some 9M HCl was add as well as spike (spike was left to equilibrate to room temperature before adding and allow for equilibration within the sample). Digestions using Aqua regia (1HCl:1HNO_3), H_2O_2 and HF were carried out as required, taking to near dryness for each, except HF where complete dryness is required. Then leaching with 4M HNO_3 was carried out and an $Fe(OH)_3$ scavenge using NH_3 was then carried out. The precipitate formed was washed thoroughly and dissolved in a minimum concentration HCl and transferred to a clean beaker. The solution was dried down and taken up in ~50 ml 9M HCl and a DIPE (di-isopropylether) extraction was carried out to remove any Fe within the sample. The first (chloride) column was pre-conditioned with ~20 ml of 1.2M HCl and 9M HCl. The sample was introduced to the column in 9M HCl and the Th fraction collected by washing with (2x25 ml) 9M HCl. The U fraction was eluted with 150 ml 1.2M HCl. The U fraction was taken to dryness and prepared for electrodepositioning. The Th fraction was taken to dryness and taken back up in 4M HNO_3 (approximately 50 ml) and an aluminium precipitation carried out with NH_4OH. Precipitate formed was washed well and dissolved in the minimum concentration HNO_3. The solution was then dried down and taken back up in 8M HNO_3 (approximately 50 ml) ready for the second (nitric) column. Second column was pre-conditioned with ~20 ml 1.2M HCl and 8M HNO_3. The Th sample was introduced to the column in 8M HNO_3, and rinsed with 2 x 25 ml aliquots 8M HNO_3. The Th fraction was then eluted with 100 ml 9M HCl and then the Th fraction was taken to dryness and prepared for electrodepositioning. Th is electrodeposited from the NH_4Cl solution onto a stainless steel planchette for alpha spectroscopy analysis. The planchette is placed on a sample holder of an EG&G Ortec (AMETEC) Octete alpha spectroscopy system and the sample holder is moved close to the detector face. Detectors are of 450 mm^2 surface area, 20 µm depletion depth Si surface barrier detectors with resolution better than 20 keV. The Octete has 8 chambers, each containing a detector of this type. The detector chamber is evacuated using an oil free vacuum pump and alpha spectra are recorded until sufficient counts (aim was 5,000) are obtained in all of the peaks of interest. Peak area identification and analysis is done by visual inspection of spectra and use of the EG&G programme Maestro 2. Specific activities of the nuclides are calculated on the basis of the peak areas, the known spike activity and the sample weights.

4.6 Stables isotopes; $\delta^{13}C$ and $\delta^{18}O$

The stable carbon and oxygen isotope analyses carried out at the Earth Sciences Centre, University of Gothenburg, Sweden, on 4 calcite samples were made accordingly: Samples, usually between 150 and 250 µg each, were roasted in vacuum for 30 minutes at 400°C to remove possible organic material and moisture. Thereafter, the samples were analysed using a VG Prism Series II mass spectrometer with a VG Isocarb preparation system on line. In the preparation system each sample was reacted with 100% phosphoric acid at 90°C for 10 minutes, whereupon the released CO_2 gas was analysed in the mass spectrometer. All isotope results are reported as δ per mil relative to the Vienna Pee Dee Belemnite (VPDB) standard. The analysing system is calibrated to the PDB scale via NBS-19.

5 Results

5.1 Mineralogy

Most of the samples contained fractures that have been repeatedly activated. This is evidenced by old fracture sets (often cataclasites, sealed networks, individual fractures and breccias, often with red-stained wall rock) with a certain mineralogy (often epidote, chlorite, quartz, calcite, prehnite, K-feldspar, hematite and illite, of which quartz and K-feldspar commonly belongs to wall rock fragments) that have been reactivated and sometimes cut by younger fractures. The mineralogy on the fracture surfaces of these relatively late open fractures is of certain interest for paleohydrogeological interpretations. Most of the sampled fractures contained clay minerals (corrensite and mixed layer, illite-smectite clay and illite), chlorite, hematite, pyrite, calcite and wall rock fragments such as K-feldspar, quartz, plagioclase and titanite, on their surfaces. REE-carbonate, barite, galena, fluorite, apatite, chalcopyrite, sphalerite and newly formed quartz and K-feldspar are found on the fracture surfaces of some samples. All samples are described in Appendix 1. The mineralogy identified with SEM-EDS and XRD differ somewhat because XRD samples are scraped off from the surface (underlying material, e.g. gouge and/or wall rock material, might be included), while only the uppermost layer on the fracture surfaces are investigated with SEM. The commonly identified minerals using XRD are quartz, K-feldspar, plagioclase, chlorite, calcite and mixed-layer clay (mostly corrensite). Epidote and goethite were identified in one sample each. Some of the minerals identified with SEM-EDS were not identified in the XRD measurements due to small portions of these minerals in the samples.

The fracture surface morphology varies widely between different samples but also in the same sample. The most common feature is a fairly smooth surface with minor parts of the surface being more rugged by later growth of crystal aggregates. The crystals in the smooth parts are sometimes striated (especially chlorite and clay minerals but also calcite). The crystals grown on the striated surfaces are often euhedral, e.g. cubic pyrite and fluorite and scalenohedral or equant calcite.

Most of the samples show hydrothermally altered, red-stained, wall rock adjacent to the fractures. The characteristics of this red-staining have been studied in samples from drill cores KLX04, Laxemar subarea /Drake and Tullborg 2006b/ as well as from KSH01A+B and KSH03A+B, Simpevarp subarea /Drake and Tullborg 2006c/, respectively. The red-stained rock features alteration of plagioclase, biotite and magnetite, formation of secondary albite, adularia, chlorite, prehnite and hematite, as well as small changes in chemistry and reducing capacity compared to fresh rock.

5.2 Chemistry

Results from the chemical analyses are found in Appendix 2. Samples with a high amount of chlorite and clay minerals are moderately enriched in e.g. Fe, Mg and Al and depleted in Si compared to the host rock (e.g. KLX07B 4.85–4.85 m, KLX07A 782.64–782.83 m, KLX08 772.34–772.49 m) while samples enriched in Ca compared to the host rock usually reflects high calcite contents (e.g. 13 wt.% CaO in KLX08 614.47–614.72 m).

LOI is only measured in four samples due to small sample volumes but in these samples the measured LOI values are very high 2.4, 5.6, 6 and 10 wt.% (see Appendix 2), due to a high amount hydrous fracture minerals, especially chlorite and clay minerals. Total values (84–95 wt.%) are low for the same reason. U and Th concentrations in the samples are 1.2–10.7 ppm and 0.4–13.9 ppm, respectively.

Five of the eleven samples analysed for whole rock chemistry have higher Cs concentrations (clay mineral rich samples, Cs: 3.5–21.8 ppm, see Appendix 2) than the wall rock which usually has 2–3 ppm Cs. Chondrite normalised rare earth element-patterns (REE-patterns) are shown in Figure 5-1. The REE-patterns are quite similar to the REE-patterns for the host rock (range of Ävrö granite REE-patterns is shown in Figure 5-2) but a slight enrichment of the light rare earth elements (LREE) can be observed in most samples resulting in a higher La/Yb ratio for the fracture samples compared with the host rock. Redox sensitive elements Ce and Eu are moderately depleted in a couple of samples (Ce – minor depletion in 2 samples and Eu – minor depletion in 8 samples). The Eu-depletion reflects the pattern in the host rock. The enrichment of LREE may in some samples be related to the presence of REE-carbonate (rich in LREE) on the fracture coatings, as observed in e.g. sample KLX08 218.80–218.83 m. LREE values can occasionally be quite high in calcite as well /Drake and Tullborg 2007/.

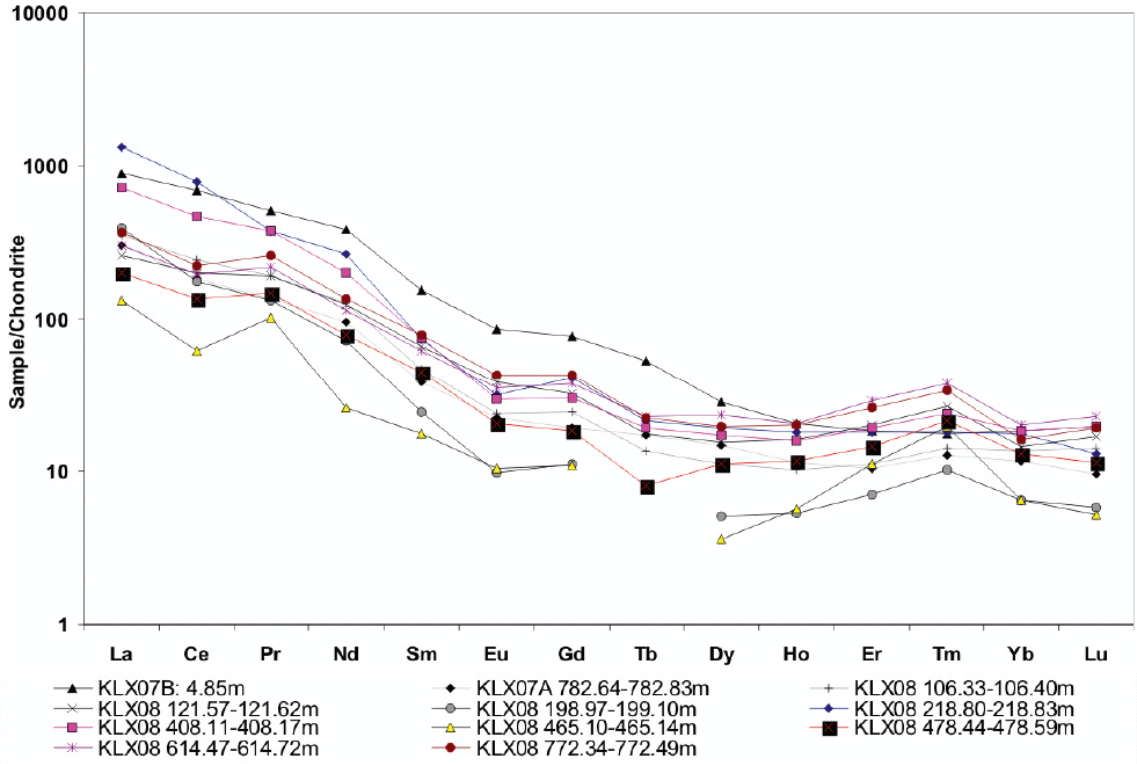

Figure 5-1. *Chondrite normalised REE-values from all of the analysed samples. Chondrite values from /Evansen et al. 1978/.*

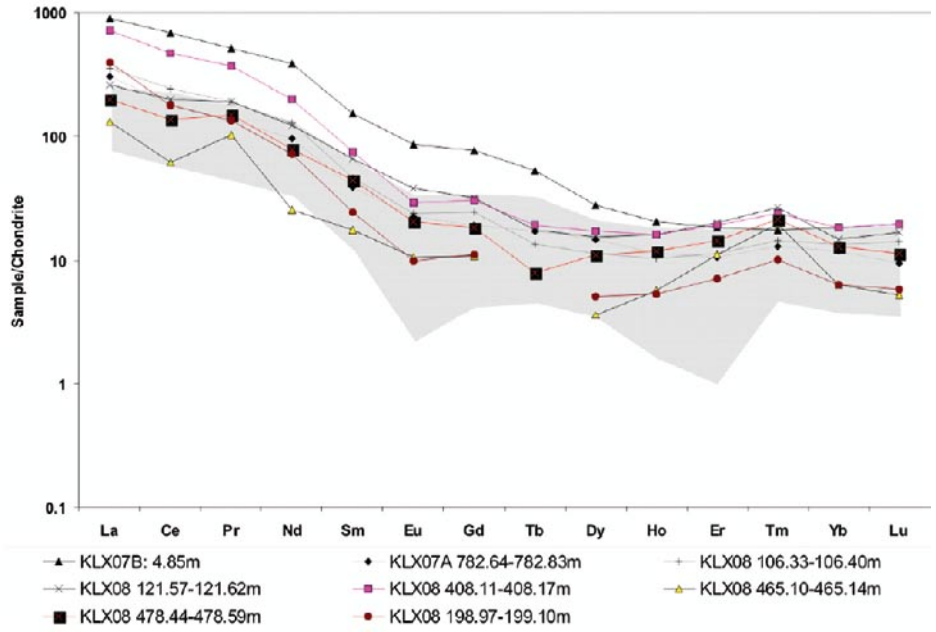

Figure 5-2. *Chondrite-normalised REE-values from samples with Ävrö granite wall rock. Maximum and minimum REE-values from a large number of fresh Ävrö granite samples is indicated with shading /Drake et al. 2006 and references there in/. Chondrite values from /Evansen et al. 1978/.*

5.3 $\delta^{13}C$ and $\delta^{18}O$

Four samples from KLX08 have been analysed for $\delta^{13}C$ and $\delta^{18}O$ in calcite. The samples are KLX08 121.57–121.62 m, KLX08 478.44–478.59 m, KLX08 852.29–852.40 m and KLX08 852.67–852.74 m and the results are found in Appendix 3.

The calcites are sampled from open or partly open fractures. Notations have been made of crystal morphology when possible since correspondence between calcite morphology (long and short c-axis) and groundwater salinity has been found in studies e.g. in Sellafield /Milodowski et al. 1998/. The indication from that study is that fresh water carbonates usually show short c-axis (nailhead shaped crystals) whereas calcite precipitated from saline waters preferably show long c-axis (scalenohedral shapes). Equant crystals are common in transition zones of brackish water. Concerning the KLX08 samples, the only sample with observable crystals shape is equant (sample KLX08 852.29–852.40 m at 732 m vertical depth).

The $\delta^{13}C$ and $\delta^{18}O$ values for the KLX08 calcites are plotted together with previously analysed calcites from the subareas Äspö, Laxemar and Simpevarp (Figure 5-3). The KLX08 calcites show $\delta^{18}O$ values ranging from –16.4 to –12.8 ‰ and $\delta^{13}C$ values from –12.5 to –9.8 ‰, which all are similar to calcite interpreted as "warm brine" precipitates /Bath et al. 2000; Tullborg 2004/. No calcite sample with low $\delta^{18}O$ and high $\delta^{13}C$, typical for hydrothermal calcites with abiogenic carbon have been found. Instead the $\delta^{13}C$ values indicate biogenic input but no signs of extreme carbon isotope fractionation (very low $\delta^{13}C$ values) typical for microbial activity during closed conditions have been found. It should be noted that the fractionation between HCO_3^- and $CaCO_3$ is only a few per mille and the $\delta^{13}C$ value in the calcite reflects therefore largely the $\delta^{13}C$ value in the bicarbonate at the time of calcite formation.

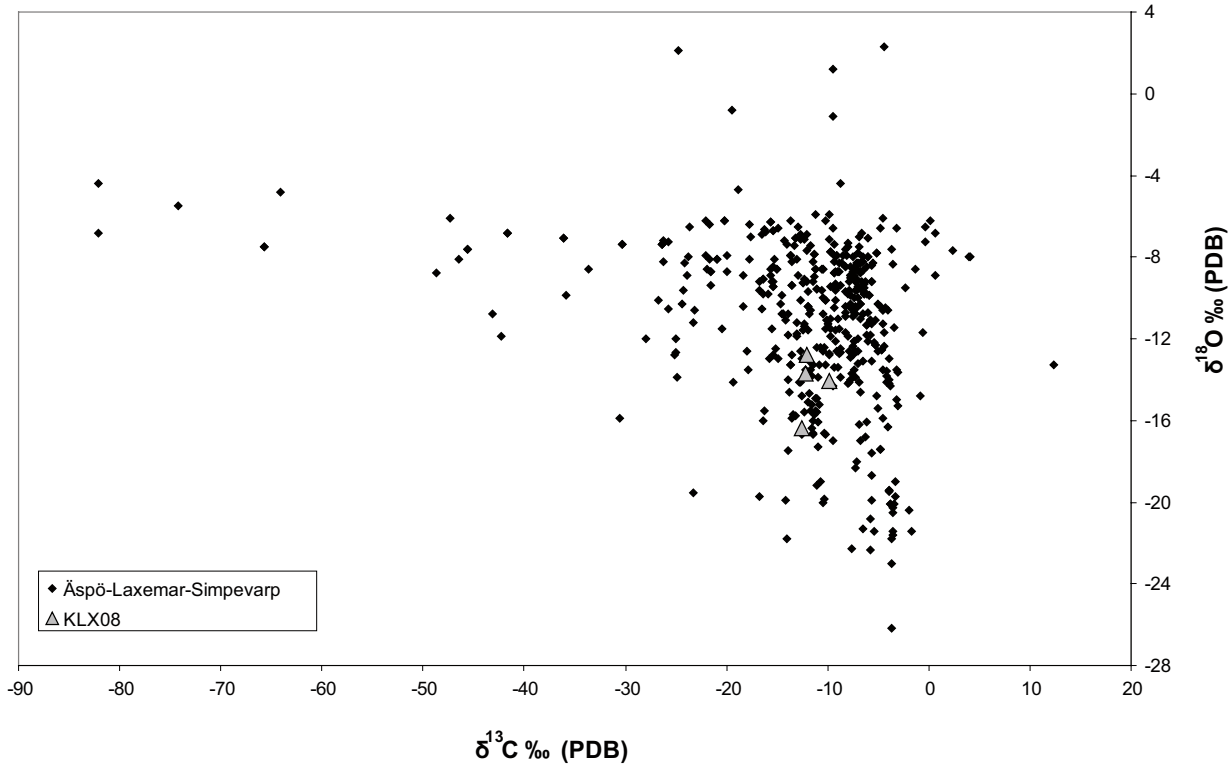

Figure 5-3. *$\delta^{13}C$ and $\delta^{18}O$ plot of calcite samples KLX08 121,57–121.62 m, KLX08 478.44–478.59 m, KLX08 852.29–852.40 m and KLX08 852.67–852.74 m, along with calcite from Äspö (e.g. KAS02, KAS03, KAS04, KAS06, KAS06, KA1755A, KR0012, KR0013, KR0015, KA3573, KA3065, KI0025F03, KA2563, KI0023F), Simpevarp(KSH01A+B, KSH02, KSH03A+B) and Laxemar (KLX01, KLX02, KLX03 and KLX04) /Wallin and Peterman 1999; Bath et al. 2000; Drake and Tullborg 2004; Milodowski et al. 2005; Drake and Tullborg 2006a; Drake and Tullborg 2007; Drake and Tullborg 2008/.*

Figures 5-4 and 5-5 show $\delta^{13}C$ and $\delta^{18}O$ plotted versus depth for KLX08 calcites (samples KLX08 121.57–121.62 m, KLX08 478.44–478.59 m, KLX08 852.29–852.40 m and KLX08 852.67–852.74 m) along with calcites from Laxemar (KLX01, KLX02, KLX03 and KLX04), Äspö (e.g. KAS02, KAS03, KAS04, KAS06, KAS06, KA1755A, KR0012, KR0013, KR0015, KA3573, KA3065, KI0025F03, KA2563, KI0023F), Simpevarp (KSH01A+B, KSH02, KSH03A+B) /Bath et al. 2000; Drake and Tullborg 2004; Milodowski et al. 2005; Drake and Tullborg 2006a; Drake and Tullborg 2007; Drake and Tullborg 2008/. These plots indicate that fractures in the upper 400 meters have been more open to low temperature circulation (possible interaction with Meteoric/Baltic sea water) and that calcites with carbon of biogenic origin, are common down to 300 m but exist also at larger depth. This is exemplified by the $\delta^{13}C$ isotope ratios from all of the KLX08 calcite samples analysed for $\delta^{13}C$ (samples KLX08 121.57–121.62 m, KLX08 478.44–478.59 m, KLX08 852.29–852.40 m and KLX08 852.67–852.74 m) which suggests that low temperature circulation might have been active as deep as 732 m (vertical depth, sample KLX08 852.29–852.40 m), in accordance with samples from e.g. KLX03 and KLX04 /Drake and Tullborg 2007; Drake and Tullborg 2008/. The distribution of calcite isotope ratios versus depth is in agreement with the flow logging results showing high hydraulic conductivity at the sampled depths. However, all of the $\delta^{18}O$ values are lower than values of Baltic water and meteoric water, which suggests that the calcites were not precipitated recently.

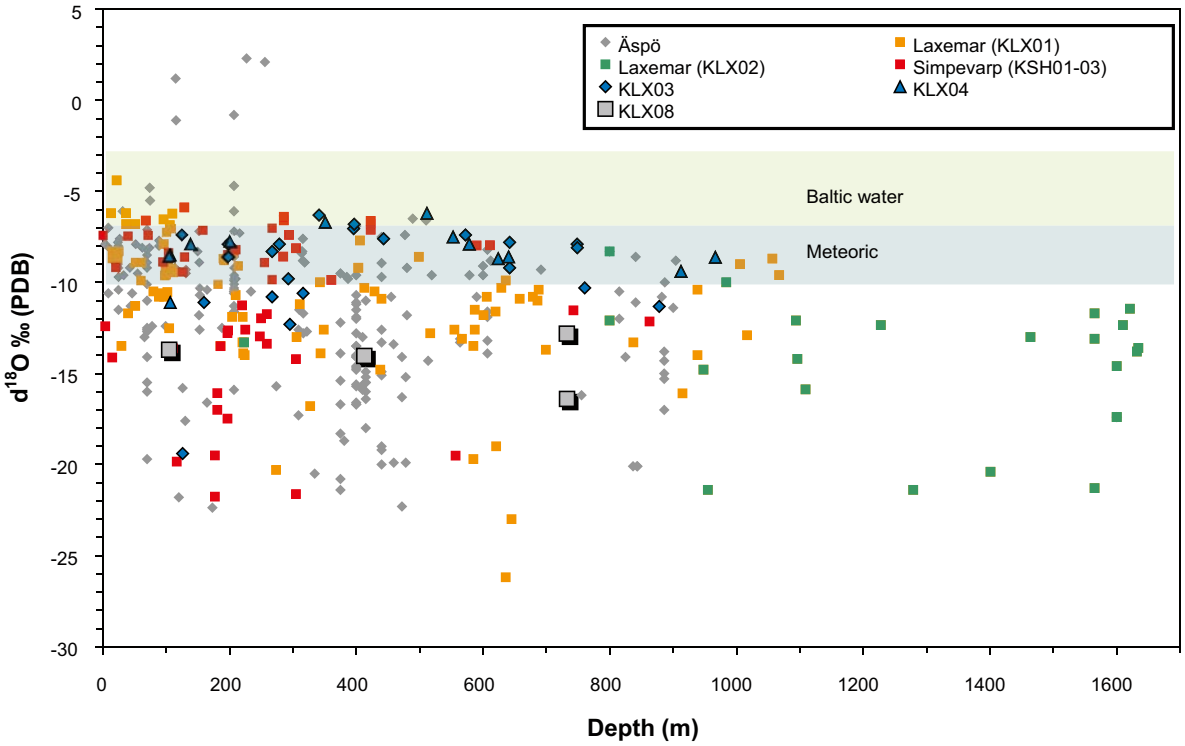

Figure 5-4. *Plot of $\delta^{18}O$ vs. depth for calcite samples KLX08 121.57–121.62 m, KLX08 478.44–478.59 m, KLX08 852.29–852.40 m and KLX08 852.67–852.74 m, along with calcite from Äspö (e.g. KAS02, KAS03, KAS04, KAS06, KAS06, KA1755A, KR0012, KR0013, KR0015, KA3573, KA3065, KI0025F03, KA2563, KI0023F), Simpevarp (KSH01A+B, KSH02, KSH03A+B) and Laxemar (KLX01, KLX02, KLX03 and KLX04) /Wallin and Peterman 1999; Bath et al. 2000; Drake and Tullborg 2004; Milodowski et al. 2005; Drake and Tullborg 2006a; Drake and Tullborg 2007; Drake and Tullborg 2008/. Range of calcite precipitated from waters similar to the present Baltic water and meteoric water at ambient temperatures is indicated – based on fractionation factors by /O'Neil et al. 1969/ and groundwater data from /SKB 2006/.*

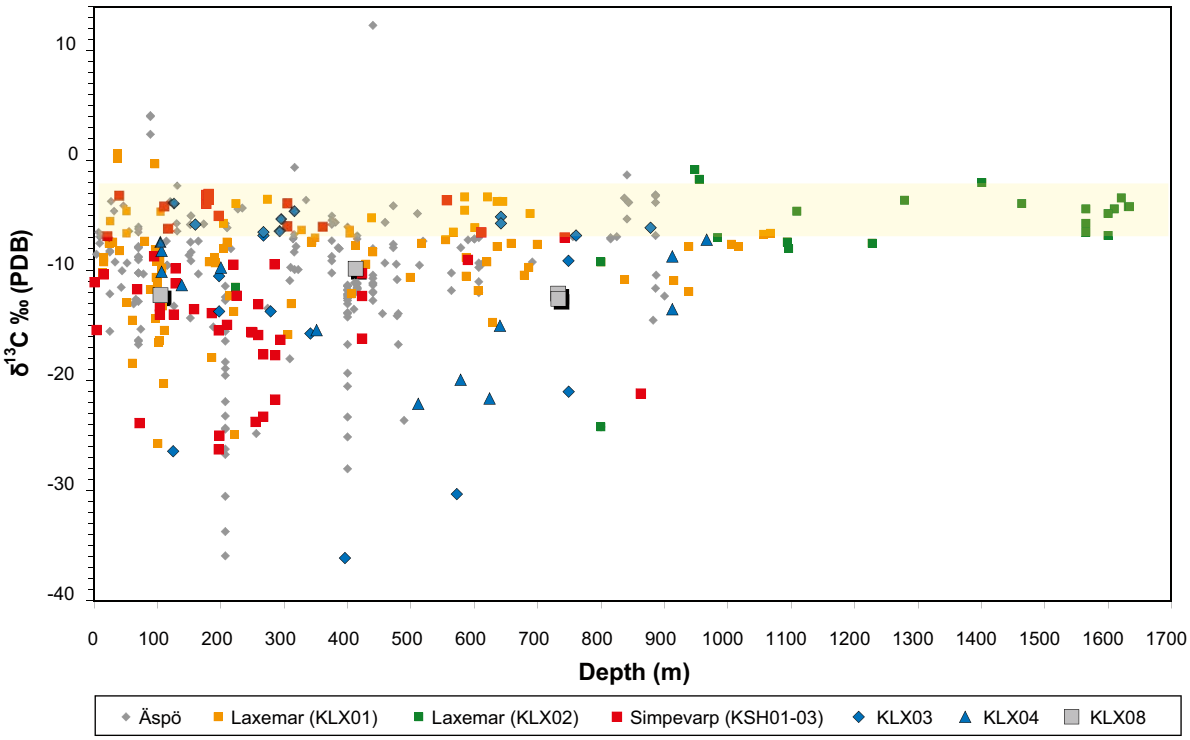

Figure 5-5. *Plot of $\delta^{13}C$ vs. depth for calcite samples KLX08 121.57–121.62 m, KLX08 478.44–478.59 m, KLX08 852.29–852.40 m and KLX08 852.67–852.74 m, along with calcite from Äspö (e.g. KAS02, KAS03, KAS04, KAS06, KAS06, KA1755A, KR0012, KR0013, KR0015, KA3573, KA3065, KI0025F03, KA2563, KI0023F), Simpevarp(KSH01A+B, KSH02, KSH03A+B) and Laxemar (KLX01, KLX02, KLX03 and KLX04) /Wallin and Peterman 1999; Bath et al. 2000; Drake and Tullborg 2004; Milodowski et al. 2005; Drake and Tullborg 2006a; Drake and Tullborg 2007; Drake and Tullborg 2008/. The shaded area indicates the range of hydrothermal inorganic CO_3^{2-} /Drake and Tullborg 2007/.*

5.4 U-series

Results of the uranium decay series analyses (USD) are presented in Appendix 4 and in Figures 5-6 and 5-7. Eight samples from KLX08 (three samples were analysed twice) and one from each of KLX07A and KLX07B have been analysed (see Table 4-1 and Appendix 4 for sample names). Comparison of the activities of U and Th obtained by U-series analyses with the ICP analyses of U and Th (shown in Appendix 2) show largely similar values (especially for U) which suggests that samples are relatively homogeneous. The $^{234}U/^{238}U$ activity ratios vary between 0.88 and 1.15 and are relatively close to one for most samples (Figure 5-6). The $^{230}Th/^{234}U$ activity ratios in contrast deviates from equilibrium (AR≈1) in many of the samples (Figure 5-6) and show generally values > 1, indicating removal of U at some stage in the past 300 ka. Three of the samples from KLX08 were re-analysed (KLX08 465.10–465.14 m, KLX08 614.47–614.72 m and KLX08 772.34–772.49 m) and the results showed large variation between the original and re-analysed samples, respectively. However, two samples (KLX08 478.44–478.59 m and KLX08 772.34–772.49 m) showed clear signs of U mobilisation probably during partly oxidising conditions. The same pattern was also obtained for sample KLX08 465.10–465.14 m. The Thiel diagram of uranium decay (Figure 5-7 /Thiel et al. 1983/) also show that samples from this study either have values close to secular equilibria or indicate mainly mobilisation of U. The samples indicating most clear signs of mobilisation are from depth below 350 m (vertical depth). The reason for this is not presently understood but disturbances during drilling and mapping needs to be taken into account. A compilation of all the U-series analyses including thorough interpretation will be carried out at a later stage, in the background report for fracture mineralogy of the Simpevarp area.

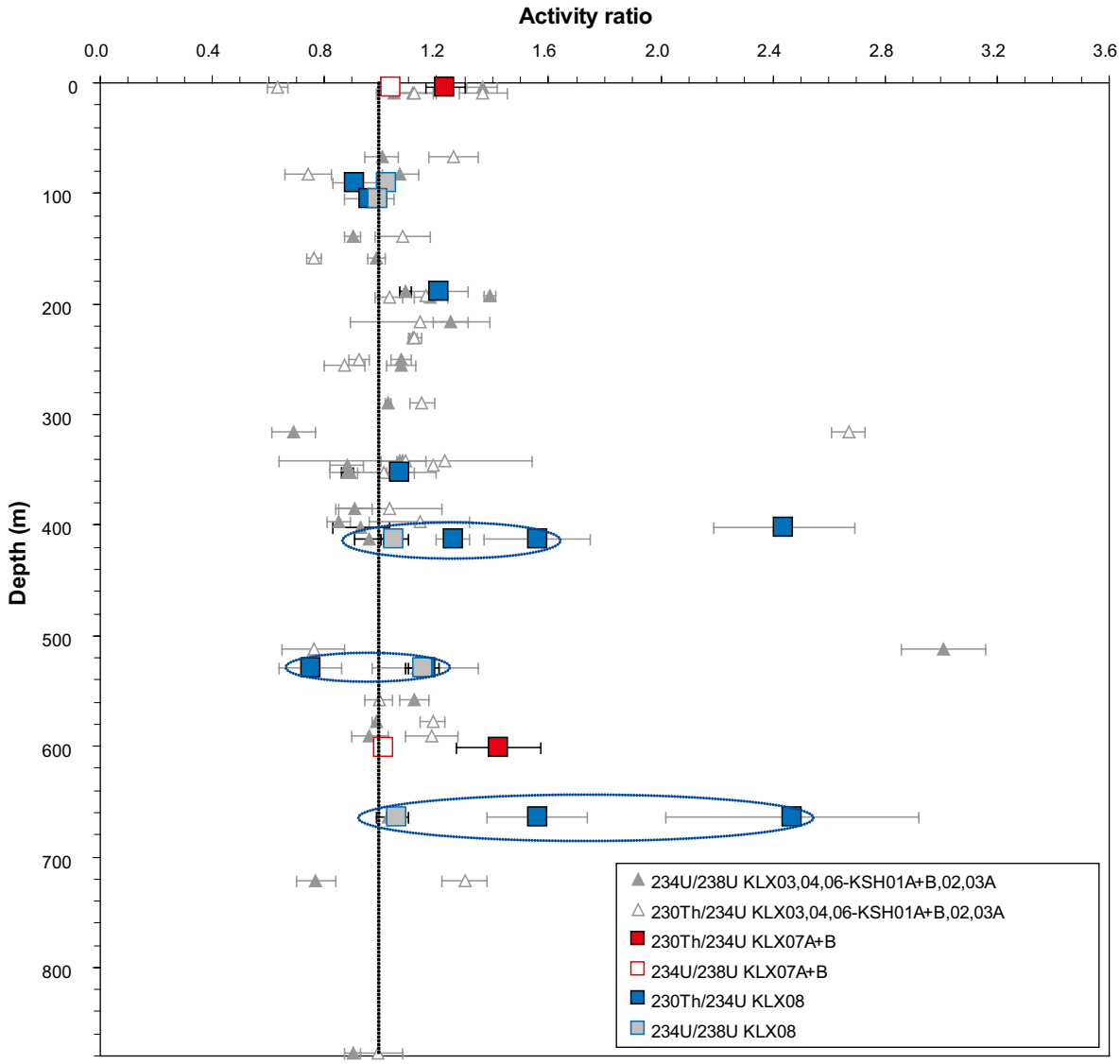

Figure 5-6. *Activity ratios of $^{234}U/^{238}U$ and $^{230}Th/^{234}U$ (with errors) vs. depth for fracture coating samples in KLX07A+B and KLX08 (KLX07B 4.85–4.85 m, KLX07A 782.64–782.83 m, KLX08 106.33–106.40 m, KLX08-121.57 121.62 m, KLX08 218.80–218.83 m, KLX08 408.11–408.17 m, KLX08 465.10–465.14 m, KLX08 478.44–478.59 m [two subsamples], KLX08 614.47–614.72 m [two subsamples], KLX08 772.34–772.49 m [two subsamples]). Re-analysed samples are within ellipses. Samples from KSH01A+B, KSH02, KSH03A, KLX03, KLX04 and KLX06 are shown for comparison /Drake and Tullborg 2008/.*

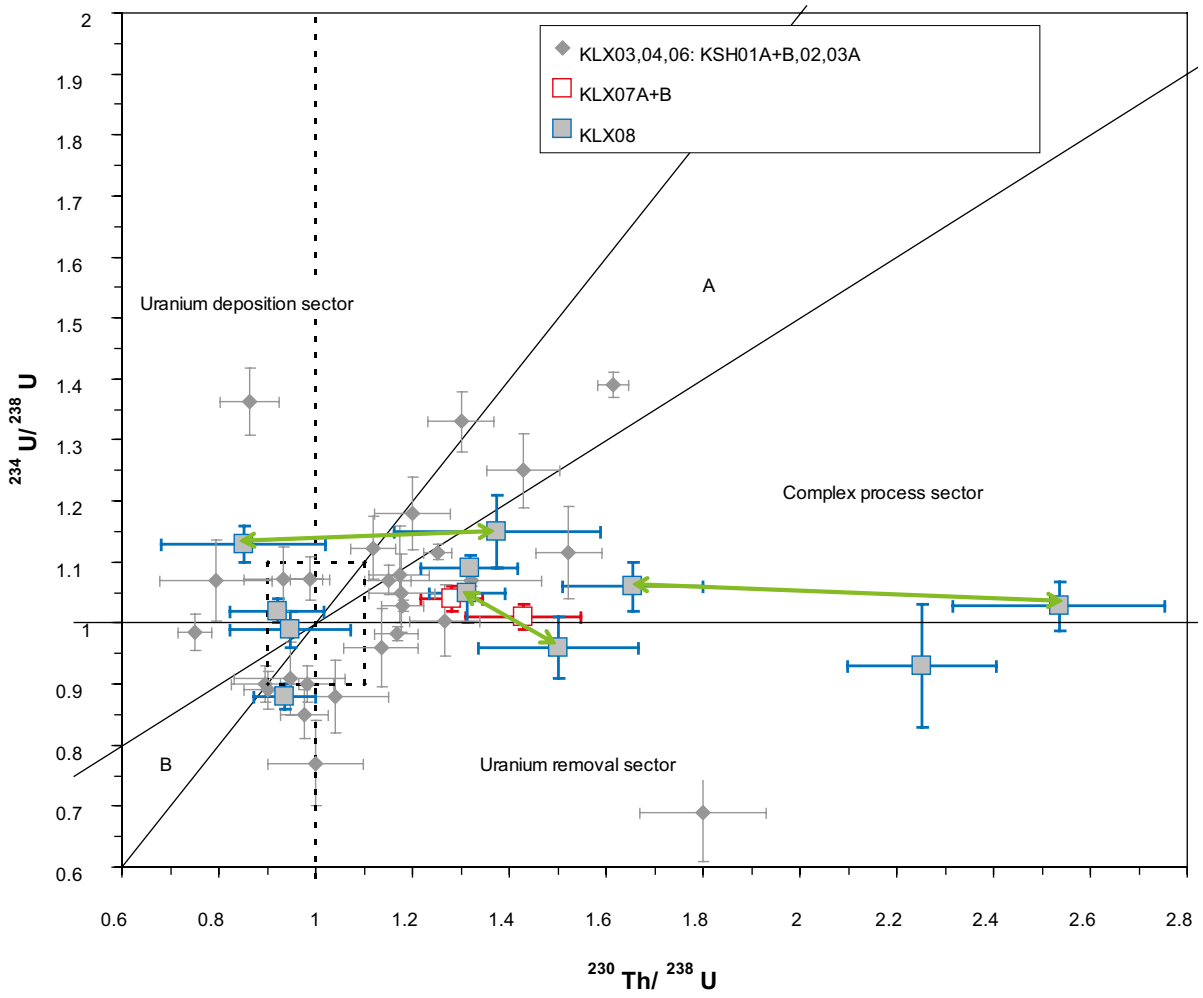

Figure 5-7. *Thiel diagram of uranium decay series for samples from KLX07A+B and KLX08 (KLX07B 4.85–4.85 m, KLX07A 782.64–782.83 m, KLX08 106.33–106.40 m, KLX08-121.57 121.62 m, KLX08 218.80–218.83 m, KLX08 408.11–408.17 m, KLX08 465.10–465.14 m, KLX08 478.44–478.59 m [two subsamples], KLX08 614.47–614.72 m [two subsamples], KLX08 772.34–772.49 m [two subsamples]) with errors (/Thiel et al. 1983/). Re-analysed samples are connected by a green line. Fields "A" and "B" are forbidden sections for any single continuous process. The field "Complex process sector" is forbidden for any single process. Samples from KSH01-03, KLX03, KLX04 and KLX06 are shown for comparison /Drake and Tullborg 2008/.However, one sample from KLX04 plots outside the diagram at $^{230}Th/^{238}U$ (2.28) and $^{234}U/^{238}U$ (3.0).*

6 Summary and discussions

Most of the samples in the sections sampled in KLX07A+B and in sections for complete chemical characterisation in KLX08 contained fractures that have been repeatedly activated: old fracture sets (e.g. cataclasites) with a certain mineralogy (chlorite, quartz, calcite, epidote, prehnite, K-feldspar, hematite and illite) have been re-activated and cut by younger fractures. The mineralogy of the open fracture surfaces include clay minerals (often corrensite and mixed-layer clay [illite/smectite] and illite), chlorite, hematite, pyrite, calcite and wall rock fragments such as K-feldspar, quartz and plagioclase. REE-carbonate, barite, galena, fluorite, apatite, chalcopyrite and newly formed quartz and K-feldspar are found on some fracture surfaces. Most of the sampled fractures contained clay minerals (corrensite and mixed layer, illite-smectite clay and illite).

The most common morphological feature of the fracture surfaces is a fairly smooth surface with minor parts of the surface being more rugged due to growth of later crystal aggregates, commonly consisting of calcite.

The samples in the sections sampled in KLX07A+B and for complete chemical characterisation in KLX08 usually have a high amount of chlorite and clay minerals and are therefore moderately enriched in e.g. Fe, Mg and Al and depleted in Si compared to the host rock while sample with the highest amount of calcite is enriched in Ca compared to the host rock (13 wt.% CaO in KLX08 614.47–614.72 m). Total values are low and LOI values are high (when measured) due to a high amount hydrous fracture minerals, especially chlorite and clay minerals. U and Th concentrations in all the samples are 1.2–10.7 ppm and 0.4–13.9 ppm, respectively. The REE-patterns usually show a small enrichment in the LREE compared with the range of Ävrö granite (cf. Figure 5-2).

Only one calcite sample (KLX08 478.44–478.59 m) from the sections sampled for complete chemical characterisation was analysed for $\delta^{18}O$ and $\delta^{13}C$ and these values are very similar to calcite interpreted as “warm brine“ precipitates at Laxemar and Äspö /Bath et al. 2000; Tullborg 2004/. The quite low $\delta^{13}C$ value suggests input of organic carbon.

U-series (USD) analyses indicate redistribution of U in some samples and when detected at large depth (below 350 m vertical depth) this may possibly be due to disturbances during drilling or mapping, especially when no other indicators points towards oxidising conditions. The USD analyses will be further evaluated when all USD results are available.

No suitable samples were obtained from water conducting fractures in KLX10.

References

Bath A, Milodowski A, Ruotsalainen P, Tullborg E-L, Cortés Ruiz A, Aranyossy J-F, 2000. Evidences from mineralogy and geochemistry for the evolution of groundwater systems during the quaternary for use in radioactive waste repository safety assessment (EQUIP project). EUR report 19,613.

Brindley G W, Brown G, (eds.), 1984. Crystal structures of clay minerals and their X-ray identification, Mineralogical Society of Great Britain and Ireland: Mineralogical Society Monograph 5, 495 p.

Drake H, Tullborg E-L, 2004. Oskarshamn site investigation. Fracture mineralogy and wall rock alteration, results from drill core KSH01A+B, SKB-P-04-250, Svensk Kärnbränslehantering AB

Drake H, Tullborg E-L, 2006a. Oskarshamn site investigation. Fracture mineralogy, Results from drill core KSH03A+B, P-06-03, Svensk Kärnbränslehantering AB.

Drake H, Tullborg E-L, 2006b. Oskarshamn site investigation. Mineralogical, chemical and redox features of red-staining adjacent to fractures, Results from drill core KLX04, P-06-02, Svensk Kärnbränslehantering AB.

Drake H, Tullborg E-L, 2006c. Oskarshamn site investigation. Mineralogical, chemical and redox features of red-staining adjacent to fractures, Results from drill cores KSH01A+B and KSH03A+B, P-06-01, Svensk Kärnbränslehantering AB.

Drake H, Tullborg E-L, 2007. Oskarshamn site investigation. Fracture mineralogy, Results from drill cores KLX03, KLX04, KLX06, KLX07A, KLX08 and KLX10A, SKB P-07-74, Svensk Kärnbränslehantering AB.

Drake H, Tullborg E-L, 2008. Oskarshamn site investigation, Mineralogy in water conducting zones, Results from boreholes KLX03, KLX04 and KLX06, P-08-41, Svensk Kärnbränslehantering AB.

Drake H, Sandström B, Tullborg E-L, 2006. Mineralogy and geochemistry of rocks and fracture fillings from Forsmark and Oskarshamn: Compilation of data for SR-Can, SKB R-06-109, Svensk Kärnbränslehantering AB

Drever S I, 1973. The preparation of oriented clay mineral specimens for X-ray diffraction analysis by a filter-membrane peel technique. American Mineralogist, 58, 553–554.

Evansen N M, Hamilton P J, O'Nions R K, 1978. Rare Earth Abundances in Chondritic Meteorites: Geochimica et Cosmochimica Acta, 42, 1199–1212.

Jasmund K, Lagaly G, (eds.), 1993. Tonminerale und Tone, D. Steinkopff Verlag, Darmstadt, 490 p.

Milodowski A E, Gillespie M R, Pearce J M, Metcalfe R, 1998. Collaboration with the SKB EQUIP programme; Petrographic characterisation of calcites from Äspö and Laxemar deep boreholes by scanning electron microscopy, electron microprobe and cathodoluminescence petrography, WG/98/45C: British Geological Survey, Keyworth, Nottingham.

Milodowski A E, Tullborg E-L, Buil B, Gomez P, Turrero M-J, Haszeldine S, England G, Gillespie M R, Torres T, Ortiz J E, Zacharias J, Silar J, Chvatal M, Strnad L, Sebek O, Bouch J E, Chenery S R, Chenery C, Shepherd T J, McKervey J A, 2005. Application of Mineralogical, Petrological and Geochemical tools for Evaluating the Palaeohydrogeological Evolution of the PADAMOT Study Sites., PADAMOT Project Technical Report WP2.

O'Neil J R, Clayton R N, Mayeda T K, 1969. Oxygen isotope fractionation in divalent metal carbonates: Journal of Chemistry and Physics, 51, 5547–5558.

PDF 1994. Powder diffraction file computer data base. International Centre for Diffraction Data, Park Lane, Swartmore, PA, USA, Set 1–43.

SKB 2006. Hydrogeochemical evaluation, Preliminary site description Laxemar subarea – version 1.2, SKB-R-06-12, Svensk Kärnbränslehantering AB.

Sokolnicki M, Pöllänen J, 2005. Oskarshamn site investigation. Difference flow logging of borehole KLX08. Subarea Laxemar, SKB P-05-267, Svensk Kärnbränslehantering AB.

Sokolnicki M, Rouhiainen P, 2005. Oskarshamn site investigation. Difference flow logging of boreholes KLX07A and KLX07B, SKB P-05-225, Svensk Kärnbränslehantering AB.

Thiel K, Vorwerk R, Saager R, Stupp H D, 1983. ^{235}U fission tracks and ^{238}U-series disequilibria as a means to study Recent mobilization of uranium in Archaean pyritic conglomerates: Earth and Planetary Science Letters, 65, 249–262.

Tullborg E-L, 2004. Palaeohydrogeological evidences from fracture filling minerals_ Results from the Äspö/Laxemar area. Mat. Res.Soc. Symp., v. Vol 807, p. 873–878.

Wallin, B Peterman Z, 1999. Calcite fracture fillings as indicators of Paleohydrology at Laxemar at the Äspö hard rock laboratory, southern Sweden: Applied Geochemistry, 14:7. 939–952.

Appendix 1

Sample descriptions

KLX07A: 782.64–782.83 m

Minerals in old reactivated fractures (macroscopic): Cataclasite (chlorite, clay minerals, K-feldspar, hematite and wall rock fragments) and fractures sealed with quartz, calcite, chlorite and epidote. The wall rock is red-stained due to hydrothermal alteration (alteration of plagioclase, biotite and magnetite and formation of secondary e.g. albite, adularia, chlorite, prehnite and hematite).

Minerals on the fracture surface (SEM-EDS, in order of abundance): Illite, mixed-layer clay, calcite, pyrite, K-feldspar, albite and galena.

Minerals in the material scraped off from the fracture coating (XRD): Quartz, K-feldspar, albite, calcite, chlorite and corrensite.

Photograph of drill core sample KLX07A: 782.64–782.83 m.

Photograph of one of the fracture surfaces of drill core sample KLX07A: 782.64–782.83 m.

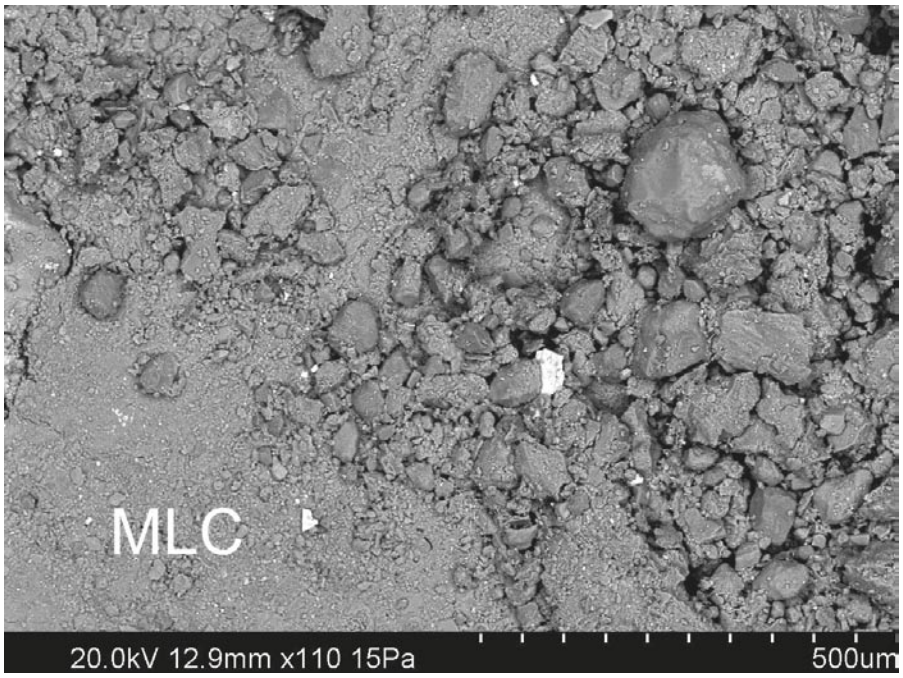

Back-scattered SEM-image of mixed layer-clay (MLC), pyrite (bright), and bigger crystals of K-feldspar, albite and illite. Sample KLX07A: 782.64–782.83 m.

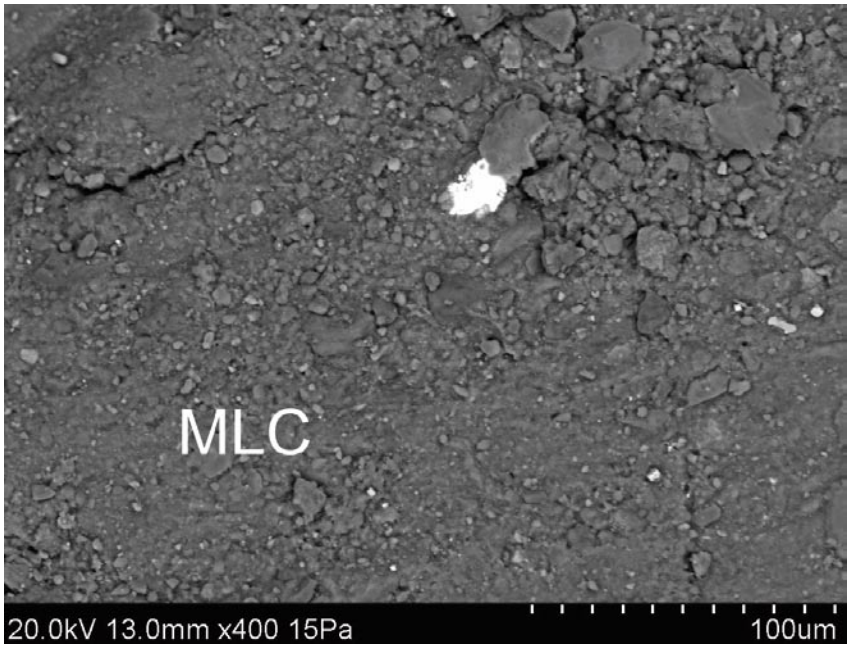

Back-scattered SEM-image of mixed layer-clay (MLC) and hematite (bright). Sample KLX07A: 782.64–782.83 m.

KLX07B: 4.85–4.85 m

Minerals in old reactivated fractures (macroscopic): Very thin filling of K-feldspar, chlorite, quartz and hematite. The wall rock is faintly red-stained close to the fracture due to hydrothermal alteration (alteration of plagioclase, biotite and magnetite and formation of secondary e.g. albite, adularia, chlorite, prehnite and hematite).

Minerals on the fracture surface (SEM-EDS, in order of abundance): Mixed layer-clay, illite, hematite, K-feldspar and trace amounts of barite.

Minerals in the material scraped off from the fracture coating (XRD): Quartz, K-feldspar, chlorite, illite and corrensite.

Photograph of drill core sample KLX07B: 4.85–4.85 m.

Photograph of the fracture surfaces of drill core sample KLX07B: 4.85–4.85 m.

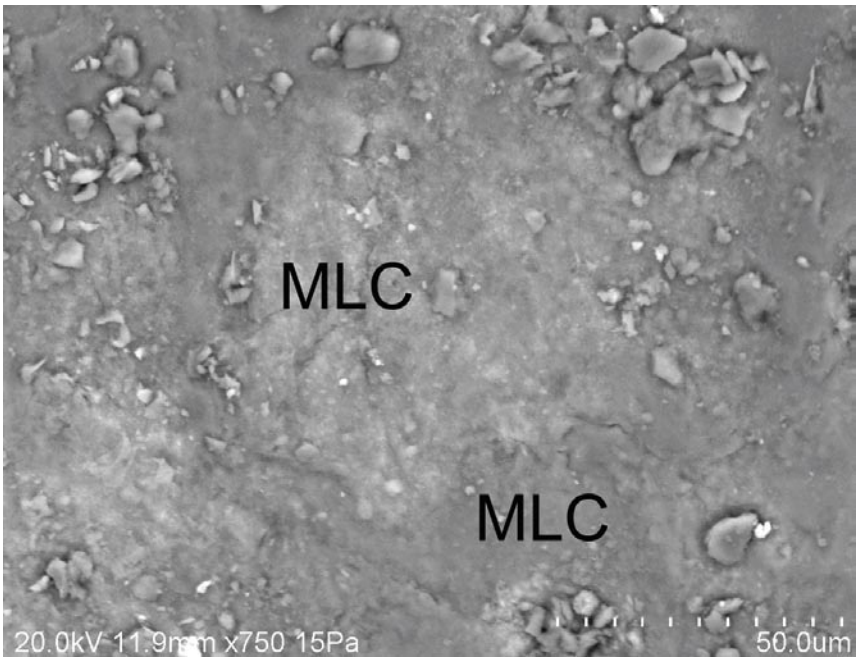

Back-scattered SEM-image of mixed layer-clay (MLC) and hematite (bright spots). Sample KLX07B: 4.85–4.85 m.

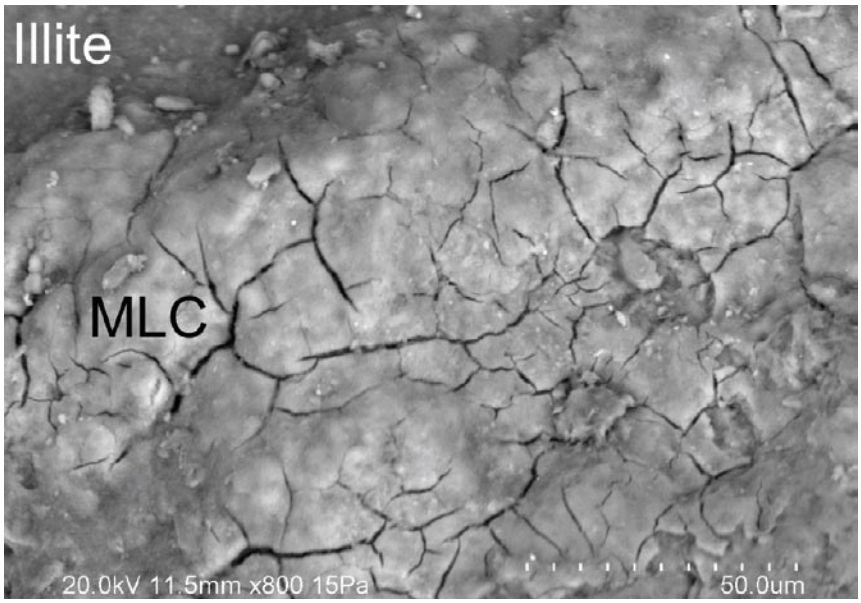

Back-scattered SEM-image of mixed layer-clay (MLC) and illite. Sample KLX07B: 4.85–4.85 m.

KLX08: 106.33–106.40 m

Minerals in old reactivated fractures (macroscopic): Calcite and cataclasite ± chlorite and prehnite. The wall rock is red-stained due to hydrothermal alteration (alteration of plagioclase, biotite and magnetite and formation of secondary e.g. albite, adularia, chlorite, prehnite and hematite). Faint bleaching of the wall rock adjacent to one of the fractures is also observed.

Minerals on fracture surface (SEM-EDS, in order of abundance): Corrensite, fine-grained wall rock fragments and trace amounts of hematite.

Minerals in the material scraped off from the fracture coating (XRD): K-feldspar, plagioclase, quartz, chlorite, illite and mixed-layer clay (probably corrensite).

Photograph of drill core sample KLX08: 106.33–106.40 m

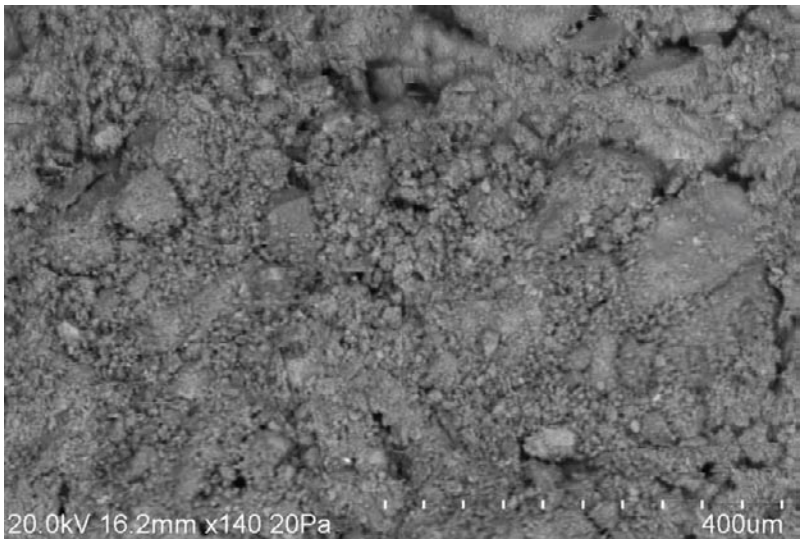

Back-scattered SEM-image of mixed-layer clay and wall rock fragments. Sample KLX08: 106.33–106.40 m.

KLX08: 121.57–121.62 m

Minerals in old reactivated fractures (macroscopic): Cataclasite, chlorite, epidote, K-feldspar, quartz and possibly hematite. The wall rock is red-stained due to hydrothermal alteration (alteration of plagioclase, biotite and magnetite and formation of secondary e.g. albite, adularia, chlorite, prehnite and hematite).

Minerals on fracture surface (SEM-EDS, in order of abundance): Dominated by mixed-layer clay, and subordinate chlorite, illite, very fine-grained wall rock fragments (e.g. zircon, titanite) and trace amounts of barite.

Minerals in the material scraped off from the fracture coating (XRD): Chlorite, quartz, K-feldspar, plagioclase, goethite, illite and small amounts of mixed-layer clay.

Photograph of drill core sample KLX08: 121.57–121.62 m.

KLX08: 198.97–199.10 m

Minerals in old reactivated fractures (macroscopic): No visible fill, some sealed fractures (sealed network) exist in the wall rock.

Minerals on fracture surface (SEM-EDS, in order of abundance): Dominated by mixed layer-clay (probably corrensite), illite and Fe-rich chlorite. Smaller amounts of albite and hematite as well as trace amounts of REE-carbonate, pyrite and an unidentified mineral rich in Cu and Zn are also present.

Photograph of drill core sample KLX08: 198.97–199.10 m.

Photograph of the fracture surfaces of drill core sample KLX08: 198.97–199.10 m.

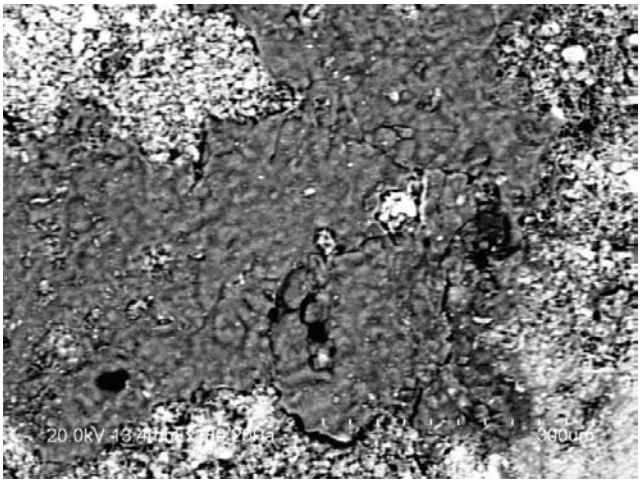

Back-scattered SEM-image of mixed-layer clay (bright) and illite (dark). Sample KLX08: 198.97–199.10 m.

Back-scattered SEM-image of mixed-layer clay. Sample KLX08: 198.97–199.10 m.

KLX08: 218.80–218.83 m

Minerals in old reactivated fractures (macroscopic): Possibly epidote, quartz, calcite, chlorite etc (thin fractures). The wall rock is red-stained due to hydrothermal alteration (alteration of plagioclase, biotite and magnetite and formation of secondary e.g. albite, adularia, chlorite, prehnite and hematite).

Minerals on fracture surface (SEM-EDS, in order of abundance): Chlorite (also in unidentified mixed layer-clay), illite, K-feldspar, titanite, REE-carbonate, quartz and hematite. An unidentified Cr-rich mineral and apatite are found in trace amounts.

Minerals in the material scraped off from the fracture coating (XRD): Quartz, K-feldspar, plagioclase, calcite, chlorite, illite and mixed-layer clay (probably dominantly of corrensite-type).

Photograph of drill core sample KLX08: 218.80-218.83 m.

KLX08: 347.99–348.15 m

Minerals in old reactivated fractures (macroscopic): Calcite (very thin undulating veins)

Minerals on fracture surface (SEM-EDS, in order of abundance): Chlorite (mostly in mixed layer-clay, probably of corrensite-type)**,** hematite, calcite, and fluorite, as well as trace amounts of REE-carbonate.

Photograph of drill core sample KLX08: 347.99–348.15 m.

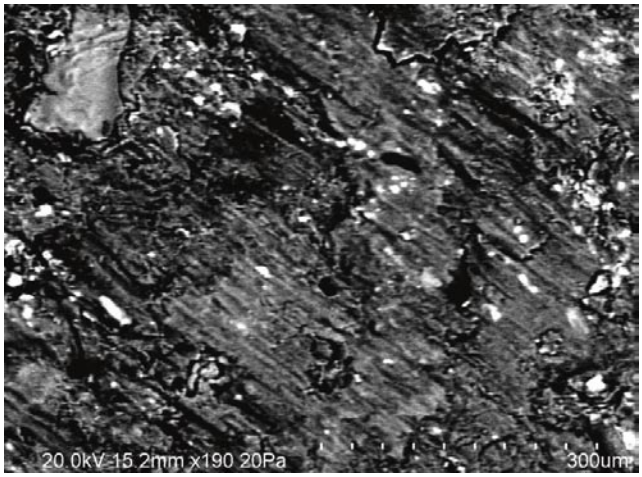

Back-scattered SEM-image of striated mixed-layer clay (dark), calcite (arrow), fluorite and hematite (both small bright crystals). Sample KLX08: 347.99–348.15 m.

KLX08: 408.11–408.17 m

Minerals in old reactivated fractures (macroscopic): Cataclasite, calcite-sealed breccia with prehnite (big fragments) and small pyrite crystals in voids.

On the fracture surface (macroscopic, in order of abundance): Chlorite, clay minerals, calcite, pyrite and hematite.

Minerals in the material scraped off from the fracture coating (XRD): Calcite, K-feldspar, plagioclase, chlorite, illite and mixed-layer clay.

Photograph of drill core sample KLX08: 408.11–408.17 m.

KLX08: 465.10–465.14 m

Minerals in old reactivated fractures (macroscopic): Prehnite, hematite (possibly with adularia and chlorite), epidote and small calcite fragments. Hematite-rich cataclasite is also present. The wall rock is red-stained due to hydrothermal alteration (alteration of plagioclase, biotite and magnetite and formation of secondary e.g. albite, adularia, chlorite, prehnite and hematite).

Minerals on fracture surface (SEM-EDS, in order of abundance): Clay minerals (chlorite in different varieties of mixed layer-clay with varied Fe content – these varieties are distinguished macroscopically by different colours, i.e. bright green or dark green), together with small amounts of pyrite and galena.

Photograph of drill core sample KLX08: 465.10–465.14 m.

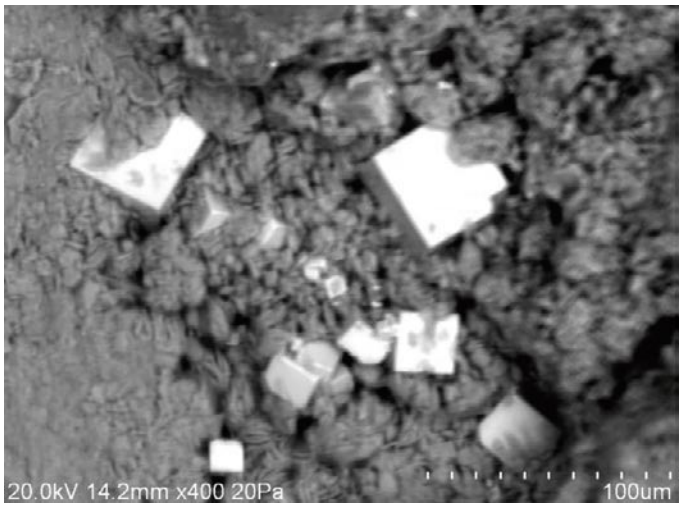

Back-scattered SEM-image of cubic pyrite crystals (bright) and mixed-layer clay (dark). Sample KLX08: 465.10–465.14 m.

Back-scattered SEM-image of two kinds of mixed layer-clay; one Fe-rich (bright) and one Mg-rich (dark). Sample KLX08: 465.10–465.14 m.

KLX08: 478.44–478.59 m

Minerals in old reactivated fractures (macroscopic): Diffuse cataclasite and some thin sealed fractures filled with prehnite, chlorite, calcite, adularia, quartz and possibly also illite and hematite. The wall rock is red-stained due to hydrothermal alteration (alteration of plagioclase, biotite and magnetite and formation of secondary e.g. albite, adularia, chlorite, prehnite and hematite).

Minerals on fracture surface (SEM-EDS, in order of abundance): Dominated by mixed-layer clay of unknown composition and illite. Other minerals are pyrite, chlorite, and trace amounts of quartz and apatite.

Minerals in the material scraped off from the fracture coating (XRD): Quartz, K-feldspar, plagioclase, chlorite, calcite, illite and mixed-layer clay.

Photograph of drill core sample KLX08: 478.44–478.59 m.

KLX08: 614.47–614.72 m

Minerals in old reactivated fractures (macroscopic): Thick calcite coating with hematite, chlorite and possibly also adularia and quartz. The wall rock is red-stained due to hydrothermal alteration (alteration of plagioclase, biotite and magnetite and formation of secondary e.g. albite, adularia, chlorite, prehnite and hematite).

Minerals on fracture surface (SEM-EDS, in order of abundance): Calcite, mixed-layer clay of unknown composition, hematite, clay minerals, chlorite, fluorite, pyrite, chalcopyrite and Zn-rich mineral.

Minerals in the material scraped off from the fracture coating (XRD): Calcite, chlorite, plagioclase, K-feldspar, illite and small amounts of mixed-layer clay.

Photograph of drill core sample KLX08: 614.47–614.72 m.

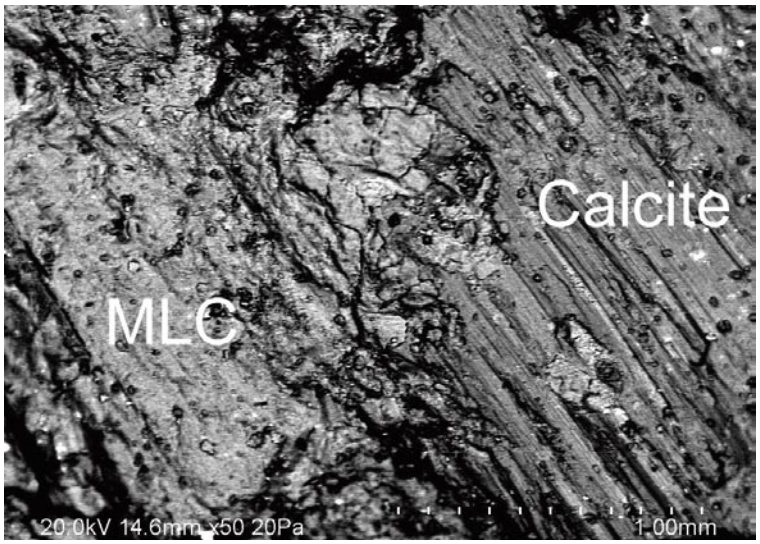

Back-scattered SEM-image of mixed layer-clay ("MLC") and striated calcite. Sample KLX08: 614.47–614.72 m.

KLX08: 772.34–772.49 m

Minerals in old reactivated fractures (macroscopic): Epidote (partly cataclastic, ± chlorite), cataclasite, calcite-sealed breccia (+K-feldspar and chlorite ± pyrite) and thin calcite-adularia-hematite-(chlorite)-veins. The wall rock is red-stained due to hydrothermal alteration (alteration of plagioclase, biotite and magnetite and formation of secondary e.g. albite, adularia, chlorite, prehnite and hematite).

Minerals on fracture surface (SEM-EDS, in order of abundance): Mixed layer-clay (probably corrensite), smaller amounts of apatite, as well as trace amounts of pyrite, sphalerite and galena.

Minerals in the material scraped off from the fracture coating (XRD): Chlorite, calcite, plagioclase, K-feldspar, quartz, epidote and corrensite.

Photograph of drill core sample KLX08: 772.34–772.49 m.

KLX08: 852.29–852.40 m

Minerals in old reactivated fractures (macroscopic): Thick calcite coating (with small amounts of quartz and chlorite) and thin calcite veins. The wall rock is faintly red-stained adjacent to the fracture.

Minerals on fracture surface (SEM-EDS, in order of abundance): Calcite (equant crystals), chlorite, mixed layer-clay, REE-carbonate, hematite and pyrite.

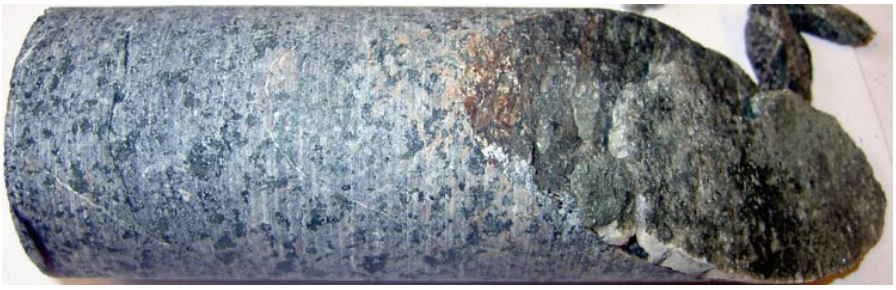

Photograph of drill core sample KLX08: 852.29–852.40 m.

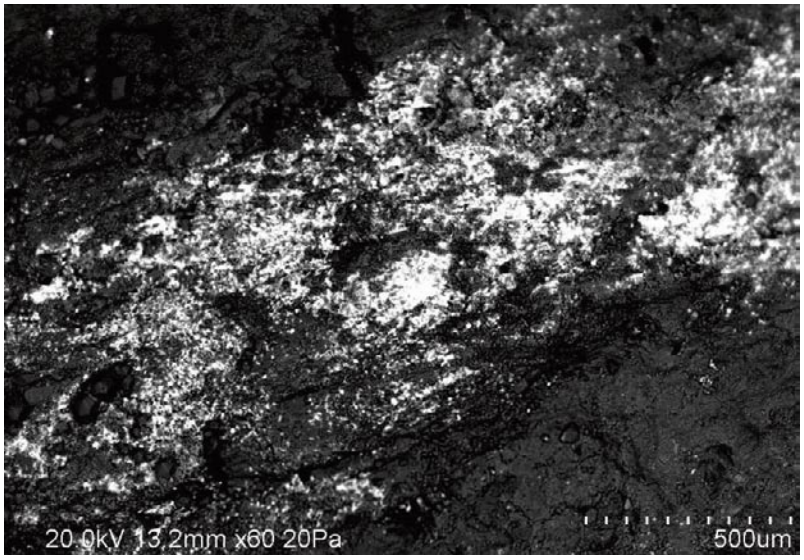

Back-scattered SEM-image of mixed layer-clay (dark) and REE-carbonate (bright). Sample KLX08: 852.29–852.40 m.

KLX08: 852.67–852.74 m

Minerals in old reactivated fractures (macroscopic): Thin sealed fracture filled with calcite, hematite and quartz. The wall rock is faintly red-stained close too the fractures.

Minerals on fracture surface (SEM-EDS, in order of abundance): Hematite, illite and chlorite (mixed-layer clay; probably of corrensite-type).

Photograph of drill core sample KLX08: 852.67–852.74 m.

Photograph of the fracture surfaces of drill core sample KLX08: 852.67–852.74 m.

Appendix 2

XRD and ICP-AES/QMS results

In this section the results from XRD and ICP-AES/QMS analyses of fracture fillings/coatings are presented. The analyses were carried out by SGU (XRD) and Analytica AB (ICP-AES/QMS).

Borehole		**KLX07B**	**KLX07A**	**KLX08**	**KLX08**	**KLX08**	**KLX08**
Length (m)		**4.85–4.85**	**782.64–782.83**	**106.33–106.40**	**121.57–121.62**	**198.97–199.10**	**218.80–218.83**
Minerals		**qz, kfs,**	**qz, kfs, ab**	**kfs, pl, qz, chl**	**chl, qz, kfs, pl**	**Not analysed**	**qz, kfs, pl, cc,**
(XRD)		**chl, ill, cor**	**cc, chl, corr**	**ill, mlc (cor)**	**gt, ill, (mlc)**		**chl, ill, mlc (cor)**
SiO_2	%	49.5	54.1	51.9	49.3	48.1	59.5
Al_2O_3	%	17.1	15.6	16.2	17.1	15.6	14.1
CaO	%	2.14	3.57	4.87	5.74	3.75	3.78
Fe_2O_3	%	8.87	6.27	5.5	7.32	9.1	3.3
K_2O	%	5.28	4.43	6.71	4.41	6.41	5.74
MgO	%	7.88	7.28	3.04	4.35	3.7	1.8
MnO	%	0.261	0.163	0.114	0.155	0.153	0.0904
Na_2O	%	2.08	2.65	2.71	2.49	0.773	2.92
P_2O_5	%	0.314	0.217	0.317	0.416	0.0907	0.177
TiO_2	%	0.676	0.663	0.735	1.09	0.187	0.547
Total	%	94.1	94.9	92.1	92.4	87.9	92
LOI	%	n.a.	n.a.	n.a.	n.a.	n.a.	2.4
Ba	mg/kg	1,750	618	2,210	1,200	581	1,280
Be	mg/kg	75.2	7.31	5.39	4.95	8.69	2.3
Co	mg/kg	36.5	6.58	13.9	19.8	< 6	< 6
Cr	mg/kg	34.4	< 10	43.2	124	225	105
Cs	mg/kg	12.1	1.23	3.58	1.65	21.8	2.34
Cu	mg/kg	460	14.5	27.8	29.2	24.3	17.7
Ga	mg/kg	29.2	19.4	16.4	31.6	24.8	11.8
Hf	mg/kg	3.72	4.96	4.18	5.47	1.5	6.1
Mo	mg/kg	< 2	< 2	< 2	< 2	< 2	< 2
Nb	mg/kg	5.22	12.5	7.79	14.1	4.27	12.9
Ni	mg/kg	35.8	< 10	20.7	34.7	12.3	< 10
Rb	mg/kg	137	87.9	185	142	254	121
Sc	mg/kg	16.7	7.12	7.66	15.4	3.08	5.91
Sn	mg/kg	7.67	11.2	1.88	4.04	1.28	2.41
Sr	mg/kg	485	590	1,000	2,710	145	286
Ta	mg/kg	0.593	1	0.796	1.08	0.39	1.36
Th	mg/kg	8.31	13.9	3.37	5.64	1.33	5.29
U	mg/kg	10.7	6.85	4.48	5.73	2.82	3.13
V	mg/kg	128	87.2	83.1	109	97	43.1
W	mg/kg	5.03	2.9	3.49	2.91	2.14	0.918
Y	mg/kg	44.9	22.3	21.9	28	7.61	30.5
Zn	mg/kg	1,900	559	143	153	99.4	560
Zr	mg/kg	190	227	209	275	98.8	329
La	mg/kg	220	73.5	86.7	64.2	96.3	326
Ce	mg/kg	438	117	155	128	113	499
Pr	mg/kg	49.2	13	18.5	18.5	12.9	36.5

Nd	mg/kg	182	45.1	60.8	58.4	34.4	127
Sm	mg/kg	23.6	5.94	7.21	10.2	3.74	11.4
Eu	mg/kg	4.99	1.29	1.39	2.22	0.568	1.85
Gd	mg/kg	15.6	3.96	5.03	6.54	2.26	8.41
Tb	mg/kg	1.98	0.639	0.505	0.658	< 0,1	0.795
Dy	mg/kg	7.14	3.74	2.84	3.93	1.3	4.84
Ho	mg/kg	1.15	0.639	0.585	0.906	0.304	1.01
Er	mg/kg	3.06	1.74	1.87	3.36	1.18	2.99
Tm	mg/kg	0.452	0.327	0.365	0.68	0.261	0.458
Yb	mg/kg	3.05	1.94	2.22	2.41	1.06	2.91
Lu	mg/kg	0.502	0.242	0.357	0.424	0.149	0.327

ab=albite, amp=amphibole, ba=barite, cc=calcite, chl=chlorite, cor=corrensite, ep=epidote, fl=fluorite, gt=goethite, hm=hematite, ill=illite, kfs=K-feldspar, mi= mica, mlc=Mixed layer clay, mus=muscovite, pl=plagioclase, qz=quartz

Borehole		**KLX08**	**KLX08**	**KLX08**	**KLX08**	**KLX08**
Length (m)		**408.11–408.17**	**465.10–465.14**	**478.44–478.59**	**614.47–614.72**	**772.34–772.49**
Minerals		**cc, kfs, pl, chl,**	**Not analysed**	**qz, kfs, pl, chl,**	**cc, chl, pl, kfs,**	**chl, cc, pl, kfs,**
(XRD)		**ill, mlc**		**cc, ill, mlc**	**ill, (mlc)**	**qz, ep, cor**
SiO_2	%	44.3	40.9	55.9	38.8	39.6
Al_2O_3	%	15.9	14.6	13.7	13	15
CaO	%	6.55	6.26	2.67	13	8.94
Fe_2O_3	%	7.6	13.8	5.98	7.12	10.4
K_2O	%	6.6	2.75	3.53	3.38	2.59
MgO	%	5.56	5.76	4.43	3.71	7.35
MnO	%	0.272	0.192	0.122	0.287	0.299
Na_2O	%	0.924	1.18	2.6	3.26	2.34
P_2O_5	%	0.23	0.06	0.133	0.323	0.468
TiO_2	%	0.561	0.121	0.526	1	1.26
Total	%	88.5	85.6	89.6	83.9	88.2
LOI	%	5.6	n.a.	n.a.	10.6	6
Ba	mg/kg	1,150	387	871	514	381
Be	mg/kg	11.4	7.48	4.85–4.85	3.78	4.67
Co	mg/kg	13.6	< 6	6.65	18.3	39.7
Cr	mg/kg	38.7	14	138	55.1	201
Cs	mg/kg	6.96	10.5	2.38	2.76	1.52
Cu	mg/kg	300	16.2	23.8	26.1	19
Ga	mg/kg	35.4	32.4	24.6	28.2	31
Hf	mg/kg	3.78	0.601	2.68	4.59	2.97
Mo	mg/kg	< 2	< 2	< 2	< 2	2.59
Nb	mg/kg	9.12	1.97	9.58	7.87	7.82
Ni	mg/kg	19.4	< 10	16.4	12.8	89.3
Rb	mg/kg	159	121	107	102	72.9
Sc	mg/kg	10.4	2.36	4.56	14.7	19.1
Sn	mg/kg	2.99	< 1	1.83	2.32	3.65
Sr	mg/kg	1160	233	488	282	852
Ta	mg/kg	0.88	0.393	0.882	0.544	0.617
Th	mg/kg	5.34	0.7	3.48	0.408	2
U	mg/kg	7.81	4.75	4.75	1.18	2.49

V	mg/kg	144	105	68.5	127	190
W	mg/kg	1.22	0.513	1.69	2.25	2.3
Y	mg/kg	25.3	3.73	15.5	32.9	31.5
Zn	mg/kg	271	128	1,880	556	540
Zr	mg/kg	208	45.9	146	211	165
La	mg/kg	175	32.3	48.8	73.5	89.7
Ce	mg/kg	300	39.5	87.1	124	143
Pr	mg/kg	36	9.85	14.3	21.2	24.8
Nd	mg/kg	94.8	12.2	37.1	53.8	63.8
Sm	mg/kg	11.7	2.68	6.9	9.56	12.2
Eu	mg/kg	1.71	0.61	1.18	2.05	2.5
Gd	mg/kg	6.23	2.23	3.79	7.77	8.8
Tb	mg/kg	0.712	< 0,1	0.3	0.851	0.837
Dy	mg/kg	4.33	0.908	2.81	5.88	5.02
Ho	mg/kg	0.902	0.322	0.664	1.16	1.13
Er	mg/kg	3.16	1.85	2.41	4.83	4.28
Tm	mg/kg	0.613	0.505	0.552	0.973	0.871
Yb	mg/kg	3.05	1.06	2.15	3.29	2.67
Lu	mg/kg	0.502	0.131	0.289	0.574	0.482

ab=albite, amp=amphibole, ba=barite, cc=calcite, chl=chlorite, cor=corrensite, ep=epidote, fl=fluorite, gt=goethite, hm=hematite, ill=illite, kfs=K–feldspar, mi= mica, mlc=Mixed layer clay, mus=muscovite, pl=plagioclase, qz=quartz

Appendix 3

$\delta^{13}C$ and $\delta^{18}O$ analysis (calcite)

Sample (KLX08)	$\delta^{13}C$ ‰PDB	$\delta^{18}O$ ‰PDB	Crystal shape
121.57–121.62	–12.233	–13.707	Massive aggregates
478.44–478.59	–9.821	–14.04	Massive aggregates
852.29–852.40	–12.082	–12.821	Equant
852.67–852.74	–12.549	–16.405	Massive aggregates

Appendix 4

U-series analyses

Sample	^{238}U	Error 1σ	^{234}U	Error 1σ	^{230}Th	Error 1σ	^{232}Th	Error 1σ	$^{234}U/^{238}U$	Error 1σ	$^{230}Th/^{234}U$	Error 1σ
KLX07B-4.85–4.85	146	2	152	2	187	9	56.2	4.7	1.04	0.02	1.23	0.07
KLX07A-782.64–782.83	85.4	1.5	86.1	1.5	122	12	59.5	8.5	1.01	0.02	1.42	0.15
KLX08-106.33–106.40	64.7	0.8	65.8	0.8	59.6	5	28.3	3.3	1.02	0.02	0.91	0.08
KLX08-121.57–121.62	84.2	1.8	83.5	1.8	79.8	8.1	42.8	5.6	0.99	0.03	0.96	0.09
KLX08-218.80–218.83	35.6	0.5	38.8	0.5	46.9	3.9	28.5	2.9	1.09	0.02	1.21	0.1
KLX08-408.11–408.17	110	2	96.3	2	103	4.5	40.4	2.4	0.88	0.02	1.07	0.05
KLX08-465.10–465.14	69.3	5	64.1	5	156	11	56.3	6.2	0.93	0.1	2.44	0.25
KLX08-478.44–478.59(1)	69.3	3	66.6	3	104	12	48.1	7.9	0.96	0.05	1.56	0.19
KLX08-478.44–478.59(2)	67	2	70	2	88	4	35	2	1.05	0.05	1.26	0.06
KLX08-614.47–614.72(1)	20.8	0.5	23.6	0.5	17.7	2.5	10.6	1.9	1.13	0.03	0.75	0.11
KLX08-614.47–614.72(2)	16	1	19	1	22	3	11	2	1.15	0.06	1.16	0.19
KLX08-772.34–772.49(1)	29	1	31	1	48	5	26	4	1.06	0.04	1.56	0.18
KLX08-772.34–772.49(2)	25.6	0.7	26.3	0.7	64.9	12	21.6	6.1	1.03	0.04	2.47	0.45

Units: Bq kg^{-1} (except for ratios)